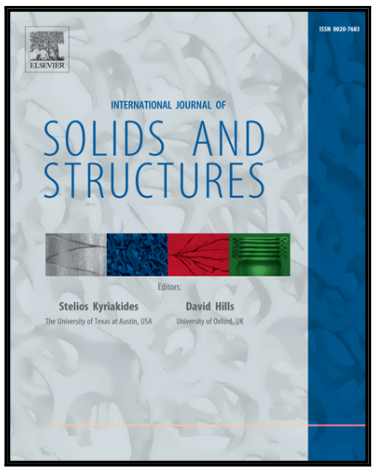

Analysis of Harmonics Propagating in Pipes of Quadratic Material Nonlinearity using Shell Theory

Yanzheng Wang , Weiqiu Chen , Jan D. Achenbach

PII: S0020-7683(17)30321-9
DOI: 10.1016/j.ijsolstr.2017.07.004
Reference: SAS 9650

To appear in: *International Journal of Solids and Structures*

Received date: 10 January 2017
Revised date: 23 May 2017
Accepted date: 3 July 2017

Please cite this article as: Yanzheng Wang , Weiqiu Chen , Jan D. Achenbach , Analysis of Harmonics Propagating in Pipes of Quadratic Material Nonlinearity using Shell Theory, *International Journal of Solids and Structures* (2017), doi: 10.1016/j.ijsolstr.2017.07.004

Analysis of Harmonics Propagating in Pipes of Quadratic Material Nonlinearity using Shell Theory

Yanzheng Wang[a,b], Weiqiu Chen[a,c], Jan D. Achenbach[b,*]

[a]Department of Engineering Mechanics, Zhejiang University, Hangzhou, 310027, China

[b]Department of Mechanical Engineering, Northwestern University, Evanston, Illinois 60208, USA

[c]Key Laboratory of Soft Machines and Smart Devices of Zhejiang Province, Zhejiang University, Hangzhou 310027, China

[*]Corresponding author at: Department of Mechanical Engineering, Northwestern University, Evanston, Illinois 60208, USA.
E-mail address: achenbach@northwestern.edu (Jan D. Achenbach)

Abstract

Higher harmonics in pipes of quadratic nonlinear material behavior have been analyzed in this paper. Using shell theory, the mixing of axisymmetric longitudinal waves and torsional waves, and the self-interaction of axisymmetric longitudinal waves, have been investigated. The dispersion curves of longitudinal waves derived from the linear version of the governing equations show excellent agreement with the corresponding curves obtained from thick shell theory and three dimensional theory, presented elsewhere. For torsional waves, only the lowest mode is taken into consideration. Using the perturbation method, analytical expressions for the resonant torsional waves generated by the mixing of longitudinal and torsional waves have been obtained. The resonant waves with difference frequencies propagate in the opposite direction of the corresponding primary wave. The back-propagation effect has potential application for nondestructive evaluation. The nonlinear shell theory is further simplified for applicability to thin pipes, to obtain expressions for the cumulative second longitudinal harmonics generated by self-interaction of longitudinal waves. For this case, the phase-match conditions, which are used to determine phase-match points, are also presented in analytical form.

Keywords: Higher harmonics; Analytical solution; Shell theory; Back-propagation; Pipe

1. Introduction

Ultrasonic waves can effectively be used to detect macroscopic defects like cracks, cavities and delaminations in an essentially linear elastic material. It is, however, important to detect damage at a smaller scale, to obtain an earlier warning of subsequent macroscale damage.

Smaller scale damage causes nonlinear material behavior which causes ultrasonic waves to generate higher harmonics. These higher harmonics can be detected to provide a measure of the microscale damage. Many experiments have confirmed the generation of higher harmonics.

Hikata *et al.* (1965) and Hikata *et al.* (1966) carried out several experiments to show the effect of dislocations on the generation of second and third harmonics in solids. Deng *et al.* (2005) and Zhang *et al.* (2014) made experimental observations of second harmonic generation of Lamb waves in an elastic plate and in long bones. Bermes *et al.* (2007) developed an effective procedure to measure the nonlinearity of metallic plates using second harmonics. The above mentioned references show that second harmonics have been frequently considered to measure the nonlinearity of materials. The quadratic terms cause, however, non-symmetry in the stresses with respect to the origin of zero stresses.

Although, higher harmonics in dispersive and non-dispersive media have attracted wide attention, including experimental, numerical and analytical investigations (Gol'dberg, 1961; Bender *et al*., 2013; Matlack *et al*. 2015; Chen *et al*.; 2014), there are few investigations of higher guided harmonics in dispersive structures like pipes and rods. Due to the dispersion of guided waves, which will lead to frequency dependent phase velocities and multi-modes, the analysis of harmonics in wave guides becomes quite complex. Recent investigations about the generation of higher guided harmonics have been made by Deng (1998, 1999), Pau and Scalea (2015) and de Lima and Hamilton (2003) by using the method of normal mode expansion. De Lima and Hamilton (2005) adopted perturbation and modal analysis together with numerical simulation to calculate the second harmonics propagating in cylindrical rods and shells. Liu *et al*. (2014a, 2014b) proposed a generalized method and used a numerical approach to analyze the cumulative nature and the physical interpretation of the generation of higher harmonics in hollow circular cylinders. Liu *et al*. (2013a) formulated a mode selection method to consider strong higher harmonics and then simulated the interaction of torsional and longitudinal waves in nonlinear circular cylinders. Nonlinear finite element models have been adopted to analyze the

cumulative second harmonics in plates and shells by Liu et al. (2013b). Chillara and Lissenden (2013) used a large radius asymptotic solution to analyze second harmonics in pipes. They concluded that only asymptotic symmetric modes can be efficiently generated from primary axisymmetric longitudinal modes. In the limits of long wavelength and weak nonlinearity, an approximate one dimensional theory was used to obtain solitons in rods (Wang *et al*., 2015a, 2015b).

Since rods and pipes are widely used in structures such as pipelines, it is highly desirable to increase our understanding of nonlinear waves propagating in cylindrical wave guides on the basis of a theory that allows relevant analytical solutions (Morsbøl and Sorokin, 2015). In this paper, we present an analytical investigation of higher harmonics in pipes based on shell theory with quadratic nonlinear material behavior. An analytical approach based on shell theory provides physical insight in the deformation modes. Whereas exact three dimensional theory has to be dealt with numerically, shell theory yields analytical solutions.

The work presented in this paper consists of three parts: the derivation of nonlinear equations of axisymmetric material behavior of a shell, the mixing of axisymmetric longitudinal and torsional waves, and the self-interaction of axisymmetric longitudinal waves. To verify the accuracy of the present linear version of the shell theory, the dispersion curves of longitudinal waves have been compared with the corresponding curves obtained from thick shell theory and three dimensional theory. For axisymmetric longitudinal wave propagation in pipes, the dispersion curves agree very well with the curves for the exact theory. For axisymmetric torsional waves, we only take the lowest torsional wave mode, derived directly from the three dimensional theory, into consideration. It is shown that for mixing of longitudinal and torsional waves, no resonant longitudinal waves with sum or difference frequency exist. Using the

perturbation method, analytical expressions for the resonant torsional waves have next been obtained. The resonant torsional waves with difference frequencies propagate in the opposite direction of the primary waves, which may have potential application to the inspection of pipes.

For the self-interaction of longitudinal waves in pipes, we have employed a more simplified shell theory for thin-walled pipes. A nonlinear displacement equation of motion with uncoupled linear part was obtained, which is used to obtain analytical expressions of cumulative second longitudinal harmonics. Since longitudinal waves according to this theory are dispersive, the phase velocities are frequency dependent. The phase-match conditions have been obtained, which, together with the dispersion relations, have been used to determine the phase-match points. At the phase-match points, the phase velocity of the second harmonic is the same as the corresponding phase velocity of the primary wave.

2. Basic equations of axisymmetric motion in a pipe derived from nonlinear shell theory

Consider a pipe of thickness h and radius of the middle surface R, see Fig. 1, where r is the distance from the middle surface, thus $\bar{r} = R + r$ is the radial position of any particle in the pipe. In this paper, axisymmetric wave propagation in the pipe will be investigated. The displacements for the shell theory are taken in the form:

$$\bar{u} = u(x,t),\ \ \bar{v} = \frac{1}{2} v(x,t)\bar{r},\ \ \ \bar{w} = w(x,t) + r\phi(x,t), \tag{1}$$

where u and w are the displacement components in the middle surface, in the radial and axial direction, respectively, and ϕ is the slope of the axial displacement in the $x-r$ plane. The forms of $\bar{u}$ and $\bar{w}$ in Eq. (1) can also be found in Herrmann and Mirsky (1956). The expression of the

circumferential displacement $\bar{v}$ in Eq. (1) is chosen to represent the lowest torsional mode, see Wang and Achenbach (2016).

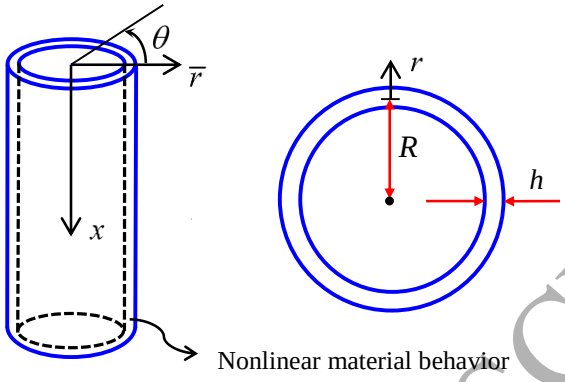

Fig. 1 (Color online) An elastic pipe

The simple form of the radial displacement given by Eq. (1_1) has advantages, but it also poses a problem in that it yields a zero radial strain, $\varepsilon_{rr} = \partial\bar{u}/\partial r = 0$. As proposed by Herrmann and Mirsky (1956), a much better assumption is that the linear radial stress is zero through the thickness of the shell, i.e.

$$\sigma_{rr}^{L} = 0 \tag{2}$$

This equation yields

$$\frac{\partial\bar{u}}{\partial r} = -\frac{\nu}{1-\nu}\left(\frac{\bar{u}}{\bar{r}} + \frac{\partial\bar{w}}{\partial x}\right) \tag{3}$$

where ν is Poison's ratio. Here the linear stress-displacement relation (Achenbach, 1999, page 74) has been used. In this paper, we use Eq. (3), except when the thickness behavior of the shell is irrelevant, when we use Eq. (1_1). Substituting Eq. (3) into the general linear axisymmetric stress-displacement relations, the resulting linear parts of stresses are

$$\sigma_{rx}^{L}=\mu\left(\frac{\partial\overline{u}}{\partial x}+\frac{\partial\overline{w}}{\partial r}\right),\quad \sigma_{\theta\theta}^{L}=2\mu\frac{\overline{u}}{\overline{r}}+\overline{\lambda}\left(\frac{\overline{u}}{\overline{r}}+\frac{\partial\overline{w}}{\partial x}\right),$$
$$\sigma_{xx}^{L}=\overline{\lambda}\left(\frac{\overline{u}}{\overline{r}}+\frac{\partial\overline{w}}{\partial x}\right)+2\mu\frac{\partial\overline{w}}{\partial x},\quad \sigma_{r\theta}^{L}=0,\quad \sigma_{\theta x}^{L}=\mu\frac{\partial\overline{v}}{\partial x} \tag{4}$$

where $\overline{\lambda}=[(1-2\nu)/(1-\nu)]\lambda$, and λ and μ are Lamé's elastic constants. The superscripts "L" and "NL" denote the linear and nonlinear parts of the stresses, respectively. The nonlinear parts of stresses are caused by the nonlinear material behavior, which is given by Eqs. (A1)-(A6) in Appendix A. Employing Eq. (3) into the nonlinear stress-displacement relations, the nonlinear parts of the stresses can be written as

$$\sigma_{rx}^{NL}=\left[\left(B-\frac{2\nu}{1-\nu}\lambda_4\right)\frac{\overline{u}}{\overline{r}}+2\frac{1-2\nu}{1-\nu}\lambda_4\frac{\partial\overline{w}}{\partial x}\right]\left(\frac{\partial\overline{w}}{\partial r}+\frac{\partial\overline{u}}{\partial x}\right) \tag{5}$$

$$\sigma_{\theta\theta}^{NL}=\lambda_1\frac{\overline{u}^2}{\overline{r}^2}+2\lambda_2\frac{\overline{u}}{\overline{r}}\frac{\partial\overline{w}}{\partial x}+\lambda_3\left(\frac{\partial\overline{w}}{\partial x}\right)^2+\frac{1}{2}B\left(\frac{\partial\overline{u}}{\partial x}+\frac{\partial\overline{w}}{\partial r}\right)^2+\lambda_4\left(\frac{\partial\overline{v}}{\partial x}\right)^2 \tag{6}$$

$$\sigma_{xx}^{NL}=\lambda_1\left(\frac{\partial\overline{w}}{\partial x}\right)^2+2\lambda_2\frac{\overline{u}}{\overline{r}}\frac{\partial\overline{w}}{\partial x}+\lambda_3\frac{\overline{u}^2}{\overline{r}^2}+\lambda_4\left[\left(\frac{\partial\overline{u}}{\partial x}+\frac{\partial\overline{w}}{\partial r}\right)^2+\left(\frac{\partial\overline{v}}{\partial x}\right)^2\right] \tag{7}$$

$$\sigma_{r\theta}^{NL}=\frac{1}{4}A\left(\frac{\partial\overline{u}}{\partial x}+\frac{\partial\overline{w}}{\partial r}\right)\frac{\partial\overline{v}}{\partial x} \tag{8}$$

$$\sigma_{\theta x}^{NL}=\left(\frac{A}{2}+\frac{1-2\nu}{1-\nu}B\right)\left(\frac{\overline{u}}{\overline{r}}+\frac{\partial\overline{w}}{\partial x}\right)\frac{\partial\overline{v}}{\partial x} \tag{9}$$

where

$$\lambda_1=A+3B+C+\frac{(3\nu-2)\nu}{(1-\nu)^2}(B+C),\quad \lambda_2=\frac{1-3\nu+3\nu^2}{(1-\nu)^2}(B+C)-\frac{\nu}{1-\nu}C,$$
$$\lambda_3=\frac{1-2\nu+2\nu^2}{(1-\nu)^2}(B+C)-\frac{2\nu}{1-\nu}C,\quad \lambda_4=\frac{A}{4}+\frac{1}{2}B \tag{10}$$

Here, *A*, *B* and *C* are the third-order elastic coefficients, and the relation $\overline{v}/\overline{r}-\overline{v}_{,r}=0$, which follows from Eq. (1_2), has been used.

Since we only take axisymmetric motion into consideration, the differential equations of motion are given by

$$\begin{aligned}
&\frac{\partial \sigma_{rr}}{\partial r}+\frac{\partial \sigma_{rx}}{\partial x}+\frac{\sigma_{rr}-\sigma_{\theta\theta}}{\bar{r}}=\rho\frac{\partial^2 \bar{u}}{\partial t^2}\\
&\frac{\partial \sigma_{r\theta}}{\partial r}+\frac{\partial \sigma_{\theta x}}{\partial x}+\frac{2\sigma_{r\theta}}{\bar{r}}=\rho\frac{\partial^2 \bar{v}}{\partial t^2}\\
&\frac{\partial \sigma_{rx}}{\partial r}+\frac{\partial \sigma_{xx}}{\partial x}+\frac{\sigma_{rx}}{\bar{r}}=\rho\frac{\partial^2 \bar{w}}{\partial t^2}
\end{aligned} \tag{11}$$

where ρ is the material density. To obtain the equations of motion for the shell, we multiply the three equations in Eq. (11) by $\bar{r}$ on each side, and then integrate the equations at both sides through the thickness of the shell. We obtain

$$\frac{\partial N_{rx}}{\partial x}-\frac{N_{\theta\theta}}{R}=\rho h\frac{\partial^2 u}{\partial t^2} \tag{12}$$

$$\frac{\partial N_{xx}}{\partial x}=\rho h\frac{\partial^2 w}{\partial t^2}+\frac{\rho h^3}{12R}\frac{\partial^2 \phi}{\partial t^2} \tag{13}$$

$$\frac{\partial N_{\theta x}}{\partial x}+\frac{N_{r\theta}}{R}=\frac{1}{2}\rho Rh\left(1+\frac{h^2}{12R^2}\right)\frac{\partial^2 v}{\partial t^2} \tag{14}$$

We also multiply the third equation in Eq. (11) by $r\bar{r}$, and integrate over the thickness of the shell to obtain

$$\frac{\partial M_x}{\partial x}-N_{rx}=\frac{\rho h^3}{12}\frac{\partial^2 \phi}{\partial t^2}+\frac{\rho h^3}{12R}\frac{\partial^2 w}{\partial t^2} \tag{15}$$

where

$$\begin{aligned}
&N_{\theta\theta}=\int_{-h/2}^{h/2}\left(\sigma_{\theta\theta}^{L}+\sigma_{\theta\theta}^{NL}\right)dr,\quad N_{xx}=\int_{-h/2}^{h/2}\left(\sigma_{xx}^{L}+\sigma_{xx}^{NL}\right)\left(1+\frac{r}{R}\right)dr,\\
&N_{rx}=\int_{-h/2}^{h/2}\left(\sigma_{rx}^{L}+\sigma_{rx}^{NL}\right)\left(1+\frac{r}{R}\right)dr,\quad M_x=\int_{-h/2}^{h/2}\left(\sigma_{xx}^{L}+\sigma_{xx}^{NL}\right)r\left(1+\frac{r}{R}\right)dr,\\
&N_{r\theta}=\int_{-h/2}^{h/2}\left(\sigma_{r\theta}^{L}+\sigma_{r\theta}^{NL}\right)dr,\quad N_{\theta x}=\int_{-h/2}^{h/2}\left(\sigma_{\theta x}^{L}+\sigma_{\theta x}^{NL}\right)\left(1+\frac{r}{R}\right)dr
\end{aligned} \tag{16}$$

Equations (12)-(15) are the equations governing axisymmetric motion of the shell. The justification for these multiplications to obtain these equations stems from energy considerations (Herrmann and Mirsky, 1956). By the use of Eqs. (4)-(9), Eq. (16) can be written as

$$N_{\theta\theta} = \left(\bar{\lambda} + 2\mu\right)\beta u + \bar{\lambda} h \frac{\partial w}{\partial x} + N_{\theta\theta}^{NL} \tag{17}$$

$$N_{xx} = (\bar{\lambda} + 2\mu)\left(h\frac{\partial w}{\partial x} + \frac{h^3}{12R}\frac{\partial \phi}{\partial x}\right) + \bar{\lambda} h \frac{u}{R} + N_{xx}^{NL} \tag{18}$$

$$M_x = (\bar{\lambda} + 2\mu)\frac{h^3}{12R}\left(\frac{\partial w}{\partial x} + R\frac{\partial \phi}{\partial x}\right) + M_x^{NL} \tag{19}$$

$$N_{rx} = \kappa\mu h(\frac{\partial u}{\partial x} + \phi) + N_{rx}^{NL} \tag{20}$$

$$N_{\theta x} = \frac{1}{2}\mu\frac{\partial v}{\partial x} Rh\left(1 + \frac{h^2}{12R^2}\right) + N_{\theta x}^{NL} \tag{21}$$

$$N_{r\theta} = N_{r\theta}^{NL} \tag{22}$$

where

$$\beta = \ln\frac{1+\bar{h}/2}{1-\bar{h}/2}, \quad \bar{h} = \frac{h}{R} \tag{23}$$

Here κ is the shear coefficient, which is introduced to modify the shear stress of the shell or plate theory. The motivation is to make the velocity of very short waves in the lowest mode coincide with the corresponding velocity of the three dimensional theory. Here κ is taken as 0.86 when the Poisson's ratio ν is 0.3 (Herrmann and Mirsky, 1956). The nonlinear parts of the resultant forces can be expressed as

$$\begin{aligned} N_{\theta\theta}^{NL} &= \int_{-h/2}^{h/2} \sigma_{\theta\theta}^{NL} dr, \quad N_{xx}^{NL} = \int_{-h/2}^{h/2} \sigma_{xx}^{NL}\left(1+\frac{r}{R}\right)dr, \quad N_{rx}^{NL} = \int_{-h/2}^{h/2} \sigma_{rx}^{NL}\left(1+\frac{r}{R}\right)dr, \\ M_x^{NL} &= \int_{-h/2}^{h/2} \sigma_{xx}^{NL} r\left(1+\frac{r}{R}\right)dr, \quad N_{r\theta} = \int_{-h/2}^{h/2} \sigma_{r\theta}^{NL} dr, \quad N_{\theta x} = \int_{-h/2}^{h/2} \sigma_{\theta x}^{NL}\left(1+\frac{r}{R}\right)dr \end{aligned} \tag{24}$$

where the nonlinear stresses are given by Eqs. (5)-(9).

Substitution of Eqs. (17)-(22) into Eqs. (12)-(15) yields the following displacement equations of motion.

$$\begin{aligned}
&\kappa\mu h\left(\frac{\partial^2 u}{\partial x^2}+\frac{\partial \phi}{\partial x}\right)-\left(\bar{\lambda}+2\mu\right)\beta\frac{u}{R}-\bar{\lambda}\bar{h}\frac{\partial w}{\partial x}-\rho h\frac{\partial^2 u}{\partial t^2}=F_1[u,\bar{v},\bar{w}]\\
&\bar{\lambda}\bar{h}\frac{\partial u}{\partial x}+(\bar{\lambda}+2\mu)h\frac{\partial^2 w}{\partial x^2}-\rho h\frac{\partial^2 w}{\partial t^2}+(\bar{\lambda}+2\mu)\frac{h^3}{12R}\frac{\partial^2 \phi}{\partial x^2}-\frac{\rho h^3}{12R}\frac{\partial^2 \phi}{\partial t^2}=F_2[u,\bar{v},\bar{w}]\\
&(\bar{\lambda}+2\mu)\frac{h^3}{12R}\frac{\partial^2 w}{\partial x^2}-\kappa\mu h\left(\frac{\partial u}{\partial x}+\phi\right)-\frac{\rho h^3}{12R}\frac{\partial^2 w}{\partial t^2}+(\bar{\lambda}+2\mu)\frac{h^3}{12}\frac{\partial^2 \phi}{\partial x^2}-\frac{\rho h^3}{12}\frac{\partial^2 \phi}{\partial t^2}=F_3[u,\bar{v},\bar{w}]\\
&\frac{1}{2}\mu Rh\left(1+\frac{h^2}{12R^2}\right)\frac{\partial^2 v}{\partial x^2}-\frac{1}{2}\rho Rh\left(1+\frac{h^2}{12R^2}\right)\frac{\partial^2 v}{\partial t^2}=F_4[u,\bar{v},\bar{w}]
\end{aligned} \tag{25}$$

where

$$F_1[u,\bar{v},\bar{w}]=\int_{-h/2}^{h/2}\left[\frac{\sigma_{\theta\theta}^{NL}}{R}-\frac{\partial \sigma_{rx}^{NL}}{\partial x}\left(1+\frac{r}{R}\right)\right]dr \tag{26}$$

$$F_2[u,\bar{v},\bar{w}]=-\int_{-h/2}^{h/2}\frac{\partial \sigma_{xx}^{NL}}{\partial x}\left(1+\frac{r}{R}\right)dr \tag{27}$$

$$F_3[u,\bar{v},\bar{w}]=\int_{-h/2}^{h/2}\left(\sigma_{rx}^{NL}-\frac{\partial \sigma_{xx}^{NL}}{\partial x}r\right)\left(1+\frac{r}{R}\right)dr \tag{28}$$

$$F_4[u,\bar{v},\bar{w}]=-\int_{-h/2}^{h/2}\left[\frac{\partial \sigma_{\theta x}^{NL}}{\partial x}\left(1+\frac{r}{R}\right)+\frac{\sigma_{r\theta}^{NL}}{R}\right]dr \tag{29}$$

Equations (26)-(29) define the nonlinear parts of Eqs. (25). If they are omitted, Eqs. (25) reduce to the linear equations governing the propagation of axisymmetric waves in a pipe.

Since Eqs. (25) are a set of nonlinear equations, the perturbation method is used to determine the effects of nonlinearity. Thus, we consider

$$u=u^{(0)}+u^{(1)},\ \bar{w}=\bar{w}^{(0)}+\bar{w}^{(1)},\ \bar{v}=\bar{v}^{(0)}+\bar{v}^{(1)} \tag{30}$$

where it is assumed that $\left|\bullet\right|^{(0)}\left| >> \right|\bullet\left|^{(1)}\right|$ and $\left|\bullet\right|^{(0)}\left|^2 \propto \right|\bullet\left|^{(1)}\right|$ are satisfied, where "$\bullet$" denotes u, $\bar{v}$ and $\bar{w}$. Based on these order of magnitude considerations, we can obtain zero-order and first-order linear governing equations. The zero-order equations are the ones presented in Eqs. (25) if the right-side terms are omitted. The first-order equations are given by

$$\begin{aligned}
&\kappa\mu h(\frac{\partial^2 u^{(1)}}{\partial x^2}+\frac{\partial \phi^{(1)}}{\partial x})-\left(\bar{\lambda}+2\mu\right)\beta\frac{u^{(1)}}{R}-\bar{\lambda}\bar{h}\frac{\partial w^{(1)}}{\partial x}-\rho h\frac{\partial^2 u^{(1)}}{\partial t^2}=F_1[u^{(0)},\bar{v}^{(0)},\bar{w}^{(0)}]\\
&\bar{\lambda}\bar{h}\frac{\partial u^{(1)}}{\partial x}+(\bar{\lambda}+2\mu)h\frac{\partial^2 w^{(1)}}{\partial x^2}-\rho h\frac{\partial^2 w^{(1)}}{\partial t^2}+(\bar{\lambda}+2\mu)\frac{h^3}{12R}\frac{\partial^2 \phi^{(1)}}{\partial x^2}-\frac{\rho h^3}{12R}\frac{\partial^2 \phi^{(1)}}{\partial t^2}=F_2[u^{(0)},\bar{v}^{(0)},\bar{w}^{(0)}]\\
&(\bar{\lambda}+2\mu)\frac{h^3}{12R}\frac{\partial^2 w^{(1)}}{\partial x^2}-\kappa\mu h(\frac{\partial u^{(1)}}{\partial x}+\phi^{(1)})-\frac{\rho h^3}{12R}\frac{\partial^2 w^{(1)}}{\partial t^2}+(\bar{\lambda}+2\mu)\frac{h^3}{12}\frac{\partial^2 \phi^{(1)}}{\partial x^2}-\frac{\rho h^3}{12}\frac{\partial^2 \phi^{(1)}}{\partial t^2}=F_3[u^{(0)},\bar{v}^{(0)},\bar{w}^{(0)}]\\
&\frac{1}{2}\mu Rh\frac{\partial^2 v^{(1)}}{\partial x^2}-\frac{1}{2}\rho Rh\frac{\partial^2 v^{(1)}}{\partial t^2}=F_4[u^{(0)},\bar{v}^{(0)},\bar{w}^{(0)}]
\end{aligned} \tag{31}$$

Here, it has been assumed that terms of orders $h^2/R^2<<1$ can be omitted.

The solutions to the zero-order equations are taken in the forms:

$$u^{(0)}=Ue^{i(\omega t-kx)},\ w^{(0)}=We^{i(\omega t-kx)},\phi^{(0)}=\frac{\Phi}{R}e^{i(\omega t-kx)},v^{(0)}=De^{i\omega(t-\frac{x}{c_T})} \tag{32}$$

where $c_T=\sqrt{\mu/\rho}$ is the shear wave velocity, ω is the circular frequency and k is the wave number. Equations (25) show that, for the axisymmetric case, linear longitudinal waves are uncoupled from linear torsional waves, as is evident from the left-side of Eq. (25_4), which is uncoupled from the linear parts of the other three equations. Substituting Eq. (32_4) into Eq. (31_4) and omitting the right side-term, the resulting equation governing torsional wave motion is satisfied by

$$\bar{v}^{(0)}=\frac{1}{2}(R+r)D\cos\omega(t-\frac{x}{c_T}) \tag{33}$$

where D is a constant. Equation (33) is the well-known representation of the lowest torsional mode in a pipe (Wang and Achenbach, 2016).

The following relations are introduced.

$$\omega = \frac{2\pi c}{\lambda},\ k = \frac{2\pi}{\lambda} \tag{34}$$

where $c = \omega/k$ is the phase velocity and λ is the wavelength. After substituting the first three expressions of Eq. (32) into the first three zero-order equations, the equations governing the relation between U, W and Φ become

$$\begin{aligned}
&\left(n^2\frac{1-\nu}{2}-\kappa\frac{1-\nu}{2}-\frac{1}{4\pi^2\delta^2}\beta\bar{h}\right)U+\nu\bar{h}i\frac{1}{2\pi\delta}W-i\kappa\frac{1-\nu}{2}\frac{1}{2\pi\delta}\bar{h}\Phi=0\\
&-\nu\bar{h}i\frac{1}{2\pi\delta}U+\left(\frac{1-\nu}{2}n^2-1\right)W=0\\
&\frac{1-\nu}{2}i\frac{1}{2\pi\delta}\kappa U+\bar{h}\left(\frac{1-\nu}{2}\frac{n^2}{12}-\frac{1-\nu}{2}\kappa\frac{1}{4\pi^2\delta^2}-\frac{1}{12}\right)\Phi=0
\end{aligned} \tag{35}$$

where $n = c/c_T$ and $\delta = h/\lambda$ are the dimensionless phase velocity and the reciprocal of dimensionless wavelength. For simplicity, the approximation has been made in the calculation that the terms containing h^3/R in the zero-order equations are negligible. The validation will be shown by comparison with the exact solution, see Fig. 2. As a consequence, part of the rotary inertia and flexural stiffness are neglected. For non-dispersive structures, the value of n equates to c_L/c_T, where $c_L = \sqrt{(\lambda+2\mu)/\rho}$ is the longitudinal wave velocity.

The determinant of the coefficient matrix of Eq. (35) must vanish, which yields the dispersion relation (also called the characteristic equation), which relates the dimensionless phase velocity and the reciprocal of the dimensionless wavelength. The dispersion curves are shown in Figs. 2a and 2b for two values of h/R.

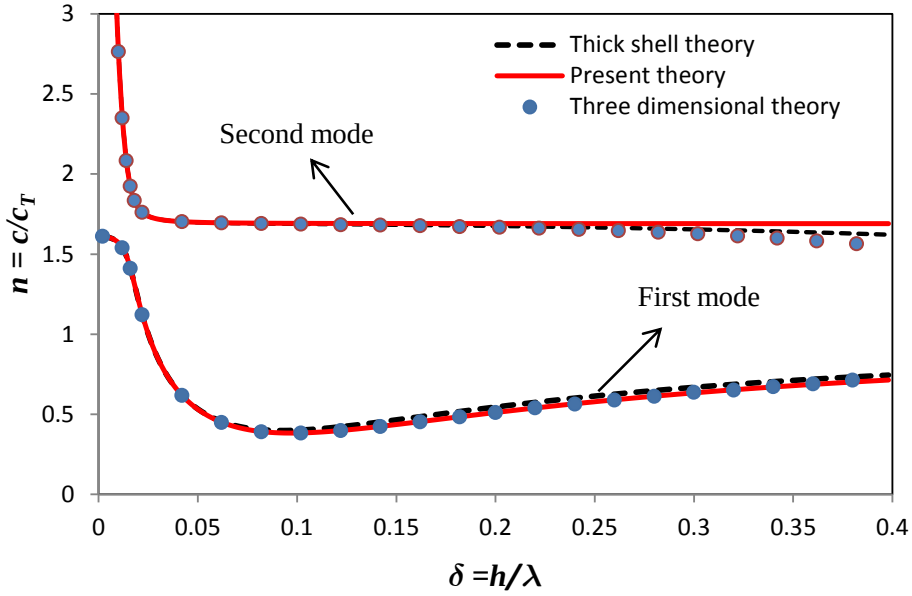

(a) $h/R = 1/10$

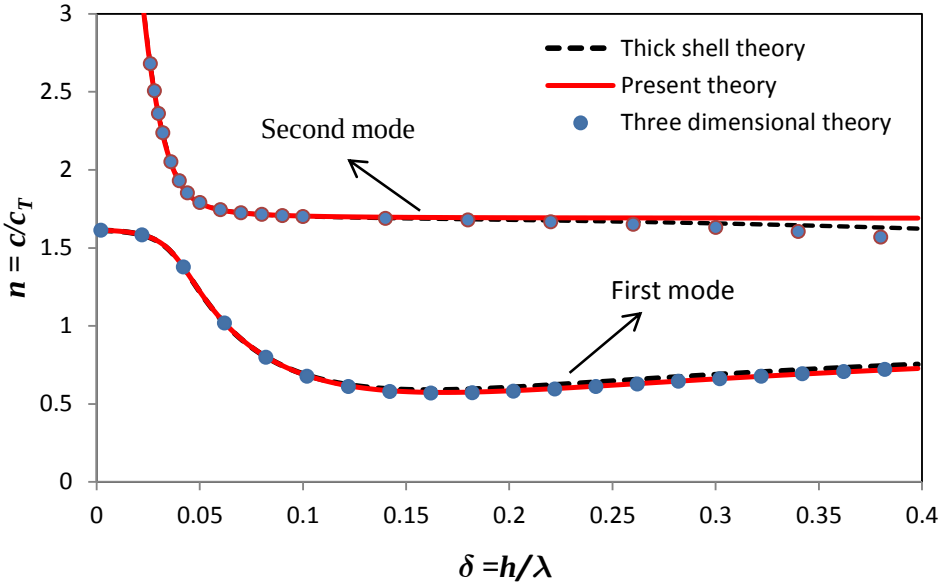

(b) $h/R = 1/4$

Fig. 2 (Color online) Comparison of phase velocity versus the reciprocal of wavelength with the corresponding results obtained from thick shell theory (Mirsky and G. Herrmann, 1958) and three dimensional theory (Herrmann and Mirsky, 1956) for $\kappa = 0.86$ and $\nu = 0.3$

Figures 2a and 2b show the comparison of the dispersion curves obtained from Eq. (35) with the ones obtained from three dimensional theory (Herrmann and Mirsky, 1956) and thick shell theory (Mirsky and G. Herrmann, 1958). When the ratio of shell thickness to wavelength is small, $h/\lambda \leq 0.4$ in this case, which can be called a lower frequency region, the dispersion curves for the first and second mode agree very well with the curves obtained from the other two theories. As the wavelength becomes smaller, the difference becomes larger for the second mode, while the first mode still remains sufficiently accurate. The results confirm that shell theory is more suitable in the lower frequency region, where the wall thickness of a pipe is sufficiently smaller than the wavelength. As shown in Li and Rose (2006), at higher frequencies (i.e. shorter wavelengths), guided waves in pipes can be treated as Lamb waves. The separation line between higher and lower frequencies depends on the ratio of the wall thickness to the diameter. Pipes of the same wall thickness with larger diameter will have a lower frequency value as the separation line. As shown in Fig. 2b, the present shell theory is still valid for fairly thick pipes. The dispersion curves show that the curve obtained from the present theory is more accurate for the first mode than the curve from the thick shell theory. One possible explanation is that the assumption used in Eq. (2) releases the restriction due to the assumed form of the displacement given by Eq. (1_1), which increases the stiffness. However, the discrepancy between three theories is very small for a small ratio of the thickness to wavelength.

We can express the radial displacement and the angle of rotation of the normal to the middle surface in terms of the axial displacement of the middle surface. The relations between the amplitudes can be obtained from Eqs. (35_2) and (35_3) as follows:

$$U = i\eta_1 W,\ \Phi = \eta_2 W \tag{36}$$

where

$$\eta_1 = -\frac{2\pi}{\nu\bar{h}}\delta\left(\frac{1-\nu}{2}n^2 - 1\right)$$

$$\eta_2 = \frac{12\pi}{\bar{h}}\frac{(1-\nu)\kappa\delta}{2\pi^2\delta^2(1-\nu)n^2 - 6(1-\nu)\kappa - 4\pi^2\delta^2}\eta_1$$

It follows that the expressions of $u^{(0)}$ and $\phi^{(0)}$ can be written as

$$\bar{u}^{(0)} = u^{(0)} = i\eta_1 w^{(0)},\ \phi^{(0)} = \frac{\eta_2}{R}w^{(0)} \tag{37}$$

We then obtain

$$\bar{w}^{(0)} = w^{(0)} + r\phi^{(0)} = (1 + \frac{r}{R}\eta_2)w^{(0)} \tag{38}$$

3. The mixing of longitudinal and torsional waves

Let us consider the case that a longitudinal wave and a torsional wave are excited at the same time. As mentioned in the previous section, these two waves will not interact with each other within the linear theory. However, when nonlinear material behavior is taken into consideration, resonant waves and higher harmonics will be generated. In this section, we are interested in investigating mixing primary longitudinal and torsional waves, to obtain a resonant wave with difference or sum frequency.

We consider the axial displacement in the middle surface in the form

$$w^{(0)} = W\cos(\omega_1 t - k_1 x) \tag{39}$$

The primary longitudinal wave with frequency ω_1 and wave number k_1 can then be determined through Eqs. (37_1) and (38) as

$$\begin{aligned} u^{(0)} &= \mathrm{Re}\left[i\eta_1 W e^{i(\omega_1 t - k_1 x)}\right] = -\eta_1 W\sin(\omega_1 t - k_1 x), \\ \bar{w}^{(0)} &= \mathrm{Re}\left[(1 + \frac{r}{R}\eta_2)e^{i(\omega_1 t - k_1 x)}\right] = (1 + \frac{r}{R}\eta_2)W\cos(\omega_1 t - k_1 x) \end{aligned} \tag{40}$$

where η_1 and η_2 are defined by:

$$\eta_1 = -\frac{2\pi}{\nu\bar{h}}\delta_1\left(\frac{1-\nu}{2}n_1^2 - 1\right) \tag{41}$$

$$\eta_2 = \frac{12\pi}{\bar{h}}\frac{(1-\nu)\kappa\delta_1}{2\pi^2\delta_1^2(1-\nu)n_1^2 - 6(1-\nu)\kappa - 4\pi^2\delta_1^2}\eta_1 \tag{42}$$

Here $\delta_1 = h/\lambda_1$, with $\lambda_1 = 2\pi/k_1$ being the wavelength of the longitudinal wave, and $n_1 = \omega_1/(k_1 c_T)$. The primary torsional wave with frequency ω_2 and wave number k_2 is given by

$$\bar{v}^{(0)} = \frac{1}{2}D(R+r)\cos(\omega_2 t - k_2 x) \tag{43}$$

where $\omega_2/k_2 = c_T$ for the lowest torsional wave mode.

It is noted that there are no terms in the expressions (26)-(28) of F_1, F_2 and F_3 containing the coupling of $\bar{v}$ with u or $\bar{w}$, which is evident by the absence of products of $\bar{v}$ with u or $\bar{w}$ in the nonlinear stress-strain relation (5)-(7). Thus, we can conclude that the mixing of primary longitudinal waves and torsional waves will not give rise to nonlinear terms with sum or difference frequency for the first three equations in Eq. (31), which govern the generation of resonant longitudinal waves. Thus, resonant longitudinal waves with sum or difference frequencies cannot occur through the mixing of primary longitudinal waves and torsional waves in a pipe. A similar conclusion that the mixing of primary transverse waves and longitudinal waves in an unbounded nonlinear media cannot give rise to a resonant longitudinal wave with difference or sum frequency, was stated in Korneev and Demčenko (2014). However, a different condition exists for the expression of F_4. Substituting Eqs, (40) and (43) into Eqs. (8), (9) and (29), we have

$$F_4 = \frac{1}{2}\mu\Psi_1 WDk^+ \sin(\omega^+ t - k^+ x) - \frac{1}{2}\mu\Psi_2 WDk^- \sin(\omega^- t - k^- x) \tag{44}$$

where $\omega^+ = \omega_1 + \omega_2$ and $\omega^- = \omega_1 - \omega_2$, also $k^+ = k_1 + k_2$ and $k^- = k_1 - k_2$, and

$$\begin{aligned}\Psi_1 &= \left(\frac{A}{2\mu} + \frac{1-2\nu}{1-\nu}\frac{B}{\mu}\right)\Psi_0 - \frac{1}{8}\frac{A}{\mu}\frac{\bar{h}\delta_2}{(\delta_1+\delta_2)}\left(\frac{2\pi\delta_1}{\bar{h}}\eta_1 + \eta_2\right), \\ \Psi_2 &= \left(\frac{A}{2\mu} + \frac{1-2\nu}{1-\nu}\frac{B}{\mu}\right)\Psi_0 - \frac{1}{8}\frac{A}{\mu}\frac{\bar{h}\delta_2}{(\delta_1-\delta_2)}\left(\frac{2\pi\delta_1}{\bar{h}}\eta_1 + \eta_2\right)\end{aligned} \tag{45}$$

where

$$\Psi_0 = -\pi\delta_2\eta_1 + 2\pi^2\frac{\delta_1\delta_2}{\bar{h}} + \frac{\pi^2\bar{h}\delta_1\delta_2}{6}(1+2\eta_2) \tag{46}$$

and $\delta_2 = h/\lambda_2$, and $\lambda_2 = 2\pi/k_2$ is the wavelength of the torsional wave. It should be noted that the special condition $\delta_1 - \delta_2 = 0$, for which the resonant wave with difference frequency does not exist, is not considered here. The quantities $\Psi_i (i = 0,\ 1,\ 2)$, as defined by Eqs. (45) and (46), defines three coefficients for the specified primary waves. In view of Eqs. (31_4) and (44), we have

$$\frac{\partial^2 v^{(1)}}{\partial x^2} - \frac{1}{c_T^2}\frac{\partial^2 v^{(1)}}{\partial t^2} = \Psi_1\frac{WDk^+}{Rh}\sin(\omega^+ t - k^+ x) - \Psi_2\frac{WDk^-}{Rh}\sin(\omega^- t - k^- x) \tag{47}$$

The resonant waves have to meet the phase-match conditions, which are given by

$$\left|\frac{\omega^-}{c_T}\right| = \left|k^-\right| \text{ or } \left|\frac{\omega^+}{c_T}\right| = \left|k^+\right| \tag{48}$$

For case one: $\left|\omega^-/c_T\right| = \left|k^-\right|$, the longitudinal phase velocity can be expressed by

$$c_1 = \frac{\omega_1}{k_1} = n_1 c_T \tag{49}$$

Then, the first resonant condition in Eq. (48) becomes

$$\frac{\omega_2}{\omega_1} = \frac{n_1 + 1}{2n_1} \tag{50}$$

For this case, we assume $n_1 \neq 1$. Thus, the wave solution to Eq. (47) will have the following form

$$v^{(1)} = a^+ \sin(\omega^+ t - k^+ x) + a^- x \cos(\omega^- t - k^- x) \tag{51}$$

Substituting Eq. (51) into Eq. (47), we can get the following equality

$$\begin{aligned} & a^+ \left(\frac{\omega^{+2}}{c_T^2} - k^{+^2} \right) \sin(\omega^+ t - k^+ x) + 2k^- a^- \sin(\omega^- t - k^- x) \\ & = \Psi_1 \frac{WDk^+}{Rh} \sin(\omega^+ t - k^+ x) - \Psi_2 \frac{WDk^-}{Rh} \sin(\omega^- t - k^- x) \end{aligned} \tag{52}$$

The values of amplitudes in Eq. (52) can then be calculated as

$$a^+ = \frac{\Psi_1 Dk^+}{R\left(\frac{\omega^{+2}}{c_T^2} - k^{+^2} \right)} \frac{W}{h}, \quad a^- = -\frac{\Psi_2 D}{2R} \frac{W}{h} \tag{53}$$

In view of Eq. (50), the phase velocities of the generated waves are given by

$$c^+ = \frac{\omega^+}{k^+} = \frac{3n_1 + 1}{3 + n_1} c_T, \; c^- = \frac{\omega^-}{k^-} = -c_T \tag{54}$$

The minus phase velocity in Eq. (54_2) means that the corresponding wave travels in the opposite direction of the primary waves. Finally, by virtue of Eqs. (51)-(54), the generated torsional wave can be expressed by

$$\bar{v}^{(1)} = \frac{1}{2}(R + r) \left[\frac{\Psi_1 WDk^+}{Rh\left(\frac{\omega^{+2}}{c_T^2} - k^{+^2} \right)} \sin \omega^+ (t - \frac{3 + n_1}{3n_1 + 1} \frac{x}{c_T}) - \frac{\Psi_2 D}{2R} \frac{W}{h} x \cos \omega^- (t + \frac{x}{c_T}) \right] \tag{55}$$

which shows that there is no cumulative behavior for the wave with sum frequency. For the wave with difference frequency the amplitude increases, however, linearly with the propagation distance. It should be noted that the waves with difference frequency propagates in the opposite direction of the primary waves. This back-propagating resonant wave may be useful for nondestructive testing purposes.

For case two: $\left|\omega^{+}/c_T\right|=\left|k^{+}\right|$, the value of n_1 must be equal to 1, which is possible for longitudinal waves propagating in pipes, see Fig. 2. The wave solution has the following form

$$v^{(1)}=a^{+}x\cos(\omega^{+}t-k^{+}x)+a^{-}x\cos(\omega^{-}t-k^{-}x) \tag{56}$$

Substituting Eq. (56) into Eq. (47) and following the analysis procedure (i.e. Eqs. (52)-(54)) used in case one, the expression of the generated torsional wave for case two is obtained as

$$\bar{v}^{(1)}=\frac{1}{2}(R+r)\left[\frac{\Psi_1 D}{2R}\frac{W}{h}x\cos\omega^{+}(t-\frac{x}{c_T})-\frac{\Psi_2 D}{2R}\frac{W}{h}x\cos\omega^{-}(t+\frac{x}{c_T})\right] \tag{57}$$

To obtain this kind of resonant waves, the phase velocity of the primary longitudinal wave c_1 has to be equal to c_T, which implies that the primary longitudinal wave has to propagate at a frequency where its velocity equals to the shear wave velocity.

The analytical expressions of resonant waves with sum and difference frequencies are shown in Eqs. (55) and (57). The coefficients Ψ_1 and Ψ_2 can be calculated through Eq. (45) for the specific primary longitudinal and torsional waves.

As examples, we determine the numerical values of Ψ_1 and Ψ_2 for several combinations of primary longitudinal and torsional waves, see Table I. The ratio of thickness to mean radius h/R is taken as $1/10$. The material constants are the same as used in Liu *et al*. (2013b), i.e.

$$\lambda=116.2\text{ GPa},\ \mu=82.7\text{ GPa},\ A=-325\text{ GPa},\ B=-310\text{ GPa},\ C=-800\text{ GPa} \tag{58}$$

The Poison's ratio ν is 0.3 and the shear coefficient κ is 0.86.

TABLE I. Values of Ψ_1 and Ψ_2 calculated from Eq. (45) for several combinations of primary torsional wave modes with the first and second modes of longitudinal waves

Group	$\delta_1=h/\lambda_1$	$n_1=\omega_1/(k_1c_T)$	$\delta_2=h/\lambda_2$	Ψ_1	Ψ_2

With the first mode of longitudinal waves					
1	0.025	1.000	0.05	1.191	1.188
2	0.1	0.383	0.05	9.717	10.101
3	0.2	0.511	0.10	44.355	48.808
4	0.3	0.633	0.15	109.220	124.499
With the second mode of longitudinal waves					
5	0.1	1.692	0.05	-4.086	-4.086
6	0.2	1.691	0.10	-16.283	-16.283
7	0.3	1.691	0.15	-36.669	-36.669

It is noted that the combination of primary waves in group 1 applies to case two (i.e. $n_1 = 1$). The analytical expressions presented in this section are not limited to the combinations in Table I. They are applicable to any combination of primary longitudinal and torsional waves, except the case that $\delta_1 = \delta_2$. It can be noted from Fig. 2 and Table I that the change of phase velocity is very small for points lying on the dispersion curve of the second longitudinal mode. This means that the dispersion effect of the longitudinal wave is weak in these regions. So the group velocity is very close to the phase velocity and the longitudinal wave is undistorted in these regions.

4. The self-interaction of longitudinal waves in a pipe

In this section, we analyze the self-interaction of axisymmetric longitudinal waves propagating in a thin-walled pipe. Compared with the equations of motion of plates in rectangular coordinates, the equations of motion of pipes in cylindrical coordinates become quite complex and require a numerical approach. Here, we will, however, investigate the second longitudinal harmonics propagating in thin-walled pipes using shell theory with nonlinear

material behavior. For thin-walled pipes, we further simplify the nonlinear governing equations (12)-(14) by neglecting rotatory inertia (the terms containing $\rho h^3/12$). We then have

$$\frac{\partial N_{rx}}{\partial x}-\frac{N_{\theta\theta}}{R}=\rho h\frac{\partial^2 u}{\partial t^2} \tag{59}$$

$$\frac{\partial N_{xx}}{\partial x}=\rho h\frac{\partial^2 w}{\partial t^2} \tag{60}$$

$$\frac{\partial M_x}{\partial x}-N_{rx}=0 \tag{61}$$

Substituting Eq. (61) into Eq. (59), we obtain

$$\frac{\partial^2 M_x}{\partial x^2}-\frac{N_{\theta\theta}}{R}=\rho h\frac{\partial^2 u}{\partial t^2} \tag{62}$$

For thin-walled pipes, we also assume that the shear deformation is very small and may be neglected, which implies

$$\varepsilon_{rx}=\frac{\partial u}{\partial x}+\frac{\partial \bar{w}}{\partial r}=0 \ \text{ or } \ \phi=-\frac{\partial u}{\partial x} \tag{63}$$

Using Eq. (63), the nonlinear stresses for longitudinal waves given by Eqs. (5)-(7) are further simplified to

$$\begin{aligned}&\sigma_{rx}^{NL}=0,\quad \sigma_{\theta\theta}^{NL}=\lambda_1\frac{u^2}{\bar{r}^2}+2\lambda_2\frac{u}{\bar{r}}\frac{\partial \bar{w}}{\partial x}+\lambda_3\left(\frac{\partial \bar{w}}{\partial x}\right)^2,\\ &\sigma_{xx}^{NL}=\lambda_1\left(\frac{\partial \bar{w}}{\partial x}\right)^2+2\lambda_2\frac{u}{\bar{r}}\frac{\partial \bar{w}}{\partial x}+\lambda_3\frac{u^2}{\bar{r}^2}\end{aligned} \tag{64}$$

In this section, the definitions of $N_{\theta\theta}^{NL}$, N_{xx}^{NL} and M_x^{NL} are the same as stated by Eq. (24), while the expressions of the nonlinear stresses (5)-(7) should be replaced by the corresponding stresses in Eq. (64). Substituting Eqs. (17)-(19) into Eqs. (60) and (62), with consideration of zero shear deformation (i.e. Eq. (63)), we obtain the displacement equations of motion as

$$(\bar{\lambda}+2\mu)\frac{h^3}{12}\frac{\partial^4 u}{\partial x^4}+\left(\bar{\lambda}+2\mu\right)\beta\frac{u}{R}+\bar{\lambda}\frac{h}{R}\frac{\partial w}{\partial x}+\rho h\frac{\partial^2 u}{\partial t^2}=\frac{\partial^2 M_x^{NL}}{\partial x^2}-\frac{N_{\theta\theta}^{NL}}{R} \tag{65}$$

$$(\bar{\lambda}+2\mu)h\frac{\partial^2 w}{\partial x^2}+\bar{\lambda}\frac{h}{R}\frac{\partial u}{\partial x}-\rho h\frac{\partial^2 w}{\partial t^2}=-\frac{\partial N_{xx}^{NL}}{\partial x} \tag{66}$$

Here, the terms containing h^2/R^2 have been neglected. The corresponding linear homogenous equations of Eqs. (65) and (66) are the Donnell's equation for axially symmetric motion of a thin shell given by Junger and Feit (1986, page 217). After some simple manipulations, Eqs. (65) and (66) can be written as two equations with uncoupled linear parts.

$$\frac{\partial w}{\partial x}=\frac{1}{\bar{\lambda}\bar{h}}\left(-\rho h\frac{\partial^2 u}{\partial t^2}-(\bar{\lambda}+2\mu)\frac{h^3}{12}\frac{\partial^4 u}{\partial x^4}-\left(\bar{\lambda}+2\mu\right)\beta\frac{u}{R}+\frac{\partial^2 M_x^{NL}}{\partial x^2}-\frac{N_{\theta\theta}^{NL}}{R}\right) \tag{67}$$

and

$$\begin{aligned}&-\rho h\frac{\partial^4 u}{\partial x^2\partial t^2}-(\bar{\lambda}+2\mu)\frac{h^3}{12}\frac{\partial^6 u}{\partial x^6}+\frac{\rho^2}{\bar{\lambda}+2\mu}h\frac{\partial^4 u}{\partial t^4}+\rho\frac{h^3}{12}\frac{\partial^6 u}{\partial t^2\partial x^4}\\&+\left(\frac{\bar{\lambda}^2}{\bar{\lambda}+2\mu}\frac{\bar{h}^2}{h}-\left(\bar{\lambda}+2\mu\right)\frac{\bar{h}}{R}\right)\frac{\partial^2 u}{\partial x^2}+\rho\frac{\bar{h}}{R}\frac{\partial^2 u}{\partial t^2}=F[u,\bar{w}]\end{aligned} \tag{68}$$

where

$$F[u,\bar{w}]=-\frac{\bar{\lambda}}{\bar{\lambda}+2\mu}\frac{\bar{h}}{h}\frac{\partial^2 N_{xx}^{NL}}{\partial x^2}+\frac{\rho}{\bar{\lambda}+2\mu}\left(\frac{\partial^4 M_x^{NL}}{\partial t^2\partial x^2}-\frac{1}{R}\frac{\partial^2 N_{\theta\theta}^{NL}}{\partial t^2}\right)-\left(\frac{\partial^4 M_x^{NL}}{\partial x^4}-\frac{1}{R}\frac{\partial^2 N_{\theta\theta}^{NL}}{\partial x^2}\right) \tag{69}$$

Note that for a thin shell (i.e. $\bar{h}<<1$), we have

$$\beta\approx\bar{h} \tag{70}$$

To solve Eq. (68), we consider in the usual manner.

$$u=u^{(0)}+u^{(1)},\quad \bar{w}=\bar{w}^{(0)}+\bar{w}^{(1)} \tag{71}$$

Substituting Eq. (71) into Eq. (68), we get a zero-order and a first-order equation. The zero-order equation is the same as Eq. (68) when the right-hand side term F is omitted.

The first-order equation is obtained as

$$-\rho h\frac{\partial^4 u^{(1)}}{\partial x^2\partial t^2}-(\bar{\lambda}+2\mu)\frac{h^3}{12}\frac{\partial^6 u^{(1)}}{\partial x^6}+\frac{\rho^2}{\bar{\lambda}+2\mu}h\frac{\partial^4 u^{(1)}}{\partial t^4}+\rho\frac{h^3}{12}\frac{\partial^6 u^{(1)}}{\partial t^2\partial x^4}$$
$$+\left(\frac{\bar{\lambda}^2}{\bar{\lambda}+2\mu}\frac{\bar{h}^2}{h}-\left(\bar{\lambda}+2\mu\right)\frac{\bar{h}}{R}\right)\frac{\partial^2 u^{(1)}}{\partial x^2}+\rho\frac{\bar{h}}{R}\frac{\partial^2 u^{(1)}}{\partial t^2}=F[u^{(0)},\bar{w}^{(0)}] \tag{72}$$

The solution to the zero-order equation is taken in the following form.

$$u^{(0)}=U\cos(\omega t-kx)=\mathrm{Re}\left[Ue^{i(\omega t-kx)}\right] \tag{73}$$

where "Re" denotes the real part of the quantity in the bracket. Substituting Eq. (73) into the zero-order equation, we obtain the following dispersion relation for a thin pipe.

$$-2\pi^2(1-\nu)\delta^2n^2+\pi^2(1-\nu)^2\delta^2n^4+\frac{4}{3}\pi^4\delta^4$$
$$-\frac{2}{3}\pi^4(1-\nu)n^2\delta^4-\left(\nu^2-1\right)\bar{h}^2-\frac{1-\nu}{2}\bar{h}^2n^2=0 \tag{74}$$

where n and δ are defined in Eq. (35).

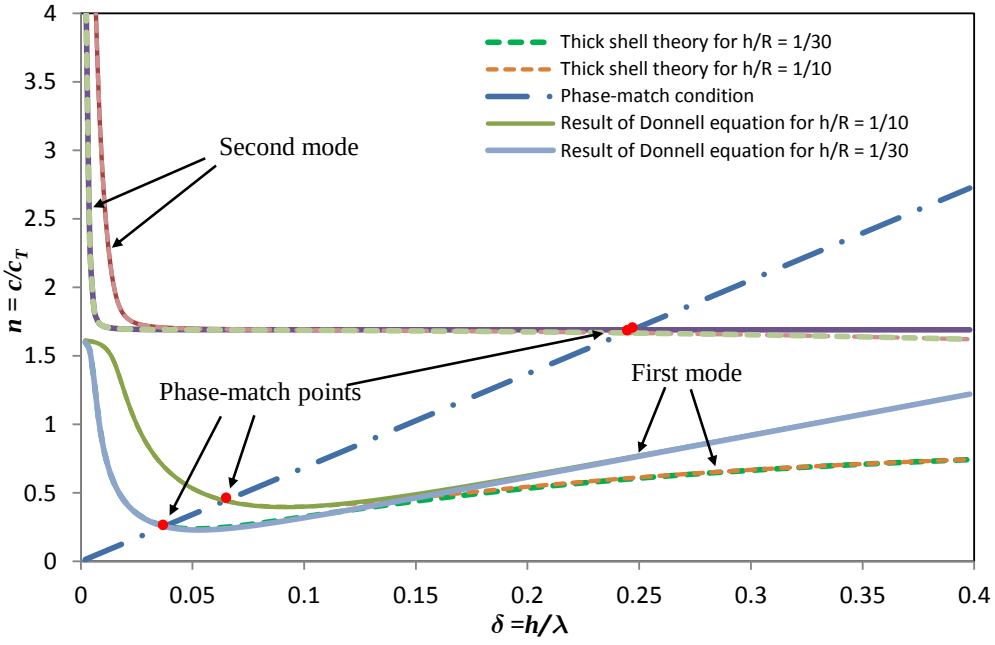

Fig. 3 (Color online) Dispersion curves and phase-match points for $\nu=0.3$

Figure 3 shows the comparison between the dispersion curves obtained from the Donnell equation and thick shell theory (Mirsky and Herrmann, 1958). When the ratio of wall thickness to wavelength is small, these two results agree very well with each other. The thick shell theory fits well with the exact theory for small values of δ, as shown in Fig. 2. Therefore, on the basis of dispersive behavior, the governing equation (68) is acceptable for waves with long wavelengths in a thin-walled pipe.

By the use of Eqs. (1_3) and (63), the following relations can be obtained.

$$\frac{\partial \bar{w}^{(0)}}{\partial r} = \phi^{(0)} = \mathrm{Re}\left[kiu^{(0)} \right] \tag{75}$$

In view of Eqs. (67) and (73), the relation between $w^{(0)}$ and $u^{(0)}$ can be written as

$$w^{(0)} = \mathrm{Re}\left[iC_1 u^{(0)} \right] \tag{76}$$

where

$$C_1 = \pi \frac{1-\nu}{\nu} \frac{1}{\bar{h}} n^2 \delta - \frac{2}{3} \pi^3 \frac{1}{\nu} \frac{1}{\bar{h}} \delta^3 - \frac{1}{2\pi} \frac{1}{\nu} \bar{h} \frac{1}{\delta} \tag{77}$$

We can then express the axial displacement by

$$\bar{w}^{(0)} = iC_1 u^{(0)} + ikru^{(0)} = \mathrm{Re}\left[i\left(C_1 + kr\right) u^{(0)} \right] \tag{78}$$

Using Eqs. (73) and (78), together with Eqs. (24) and (64), the nonlinear resultant forces become

$$N_{xx}^{NL} = \Gamma_1 \lambda_2 \frac{U^2}{h} \cos^2(\omega t - kx) \tag{79}$$

$$M_x^{NL} = \Gamma_2 \lambda_2 U^2 \cos^2(\omega t - kx) \tag{80}$$

$$N_{\theta\theta}^{NL} = \Gamma_3 \lambda_2 \frac{U^2}{h} \cos^2(\omega t - kx) \tag{81}$$

where

$$\Gamma_1 = 4\pi^2 \frac{\lambda_1}{\lambda_2}\delta^2\left(C_1^{\,2} + \frac{1}{3}\pi^2\delta^2 + \frac{1}{3}\pi\bar{h}C_1\delta\right) + 4\pi C_1\bar{h}\delta + \frac{\lambda_3}{\lambda_2}\bar{h}^2,$$
$$\Gamma_2 = 4\pi^2 \frac{\lambda_1}{\lambda_2}\left(C_1^2\frac{\bar{h}}{12} + \frac{1}{3}\pi C_1\delta + \frac{1}{20}\pi^2\bar{h}\delta^2\right)\delta^2 + \frac{2}{3}\pi^2\bar{h}\delta^2, \tag{82}$$
$$\Gamma_3 = \frac{\lambda_1}{\lambda_2}\bar{h}^2 + 4\pi\bar{h}C_1\delta + \frac{\lambda_3}{\lambda_2}\left(4\pi^2C_1^2\delta^2 + \frac{4}{3}\pi^4\delta^4\right)$$

These expressions define three coefficients for the longitudinal primary wave. Substituting Eqs. (79)-(81) into Eq. (69), we obtain

$$F[u^{(0)}, \bar{w}^{(0)}]$$
$$= 4\pi^2\delta^2\lambda_2\left[\frac{2\bar{\lambda}}{\bar{\lambda}+2\mu}\bar{h}\Gamma_1 + \left(\frac{\mu}{\bar{\lambda}+2\mu}n^2 - 1\right)\left(32\Gamma_2\pi^2\delta^2 + 2\bar{h}\Gamma_3\right)\right]\frac{U^2}{h^4}\cos 2(\omega t - kx) \tag{83}$$

Let us consider a solution to Eq. (72) in the form

$$u^{(1)} = \bar{U}x\sin 2(\omega t - kx) \tag{84}$$

Substituting Eqs. (83) and (84) into Eq. (72), we get the following equation:

$$\frac{32\pi^2\delta^2\mu}{h^3(1-\nu)}\Lambda\bar{U}z\sin 2(\omega t - kz)$$
$$-\frac{16\pi\delta\mu}{h^2}\left[8\pi^2\delta^2n^2 - \frac{64}{1-\nu}\pi^4\delta^4 + \frac{64}{3}\pi^4\delta^4n^2 - \bar{h}^2(\nu+1)\right]\bar{U}\cos 2(\omega t - kz) \tag{85}$$
$$= 8\pi^2\delta^2\lambda_2\left[\nu\bar{h}\Gamma_1 + \left(\frac{1-\nu}{2}n^2 - 1\right)\left(16\Gamma_2\pi^2\delta^2 + \bar{h}\Gamma_3\right)\right]\frac{U^2}{h^4}\cos 2(\omega t - kz)$$

where

$$\Lambda = -8(1-\nu)\pi^2\delta^2n^2 + \frac{64}{3}\pi^4\delta^4 + 4\pi^2(1-\nu)^2\delta^2n^4$$
$$-\frac{32}{3}(1-\nu)\pi^4\delta^4n^2 - (\nu^2-1)\bar{h}^2 - \frac{1-\nu}{2}\bar{h}^2n^2 \tag{86}$$

Equation (85) has a solution which does not depend on time when $\Lambda = 0$, which implies

$$
\begin{aligned}
&-8(1-\nu)\pi^2\delta^2 n^2+\frac{64}{3}\pi^4\delta^4+4\pi^2(1-\nu)^2\delta^2 n^4 \\
&-\frac{32}{3}(1-\nu)\pi^4\delta^4 n^2-(\nu^2-1)\bar{h}^2-\frac{1-\nu}{2}\bar{h}^2 n^2=0
\end{aligned}
\tag{87}
$$

Since $\Lambda=0$, we can obtain the amplitude of the second longitudinal harmonic, Eq. (84), from Eq. (85) as

$$
\bar{U}=\Psi_3\frac{U^2}{h^2} \tag{88}
$$

where

$$
\Psi_3=\frac{\pi\lambda_2\delta\left[\nu\bar{h}\Gamma_1+\left(\frac{1-\nu}{2}n^2-1\right)\left(4\Gamma_2 4\pi^2\delta^2+\bar{h}\Gamma_3\right)\right]}{2\mu\left[-8\pi^2\delta^2 n^2-\frac{64}{3}\pi^4\delta^4 n^2+\frac{64}{1-\nu}\pi^4\delta^4+(1+\nu)\bar{h}^2\right]} \tag{89}
$$

Basically, Eq. (87), which gives the relation between 2ω and $2k$, is the dispersion relation for second harmonics. For a non-dispersive structure like an unbounded medium, the dispersion relation for the primary wave is the same as the corresponding relation for the second harmonics, and the phase velocities keep unchanged when the frequencies vary. For waves in dispersive structures, there exist only limited phase-match points where the phase velocities of primary waves are the same as the corresponding phase velocities of second harmonics. If we plot the two dispersion relations (74) and (87) in the same figure, the intersections of the two curves are phase-match points. In this paper, we obtain a relation between δ and n by subtracting Eq. (74) from Eq. (87). The resulting equation can be reduced to

$$
\left[5\pi^2\delta^2-3\left(\frac{1-\nu}{2}\right)n^2\right]\left(1-\frac{1-\nu}{2}n^2\right)=0 \tag{90}
$$

which gives rise to the following relations

$$
n=\pi\sqrt{\frac{10}{3(1-\nu)}}\delta \tag{91}
$$

and

$$n = \sqrt{\frac{2}{1-\nu}} \tag{92}$$

Equations (91) and (92) are phase-match conditions, which are independent of the ratio of the thickness to radius of a pipe. Equation (91) defines a straight line in the $\delta - n$ plane, shown in Fig. 3. The intersections of the line with the dispersion curves yield the phase-match points. The numerical values of the phase-match points have been verified by substitution in Eqs. (74) and (87). Another two phase-match points can be obtained by substitution of Eq. (92) into Eq. (74) or Eq. (87) for the two different ratios of wall thickness to mean radius considered here. For the pipes with the ratio of thickness to mean radius of 1/10 and 1/30, the phase-match point lying on the dispersion curve of the first mode is in the region of accuracy of the Donnell theory, see Fig. 3. The dispersion curves of the second harmonics are neglected in Fig. 3. Since the ratio of thickness to wavelength of the second harmonic is 2δ, the region of accuracy of the second harmonic is smaller. The phase-match points lying on the dispersion curve of the second mode are out of the accuracy region shown in Fig. 3. Considering the second longitudinal harmonics in the pipe with ratio of thickness to mean radius of 1/10 and 1/30, we can determine the phase-match points by using the present theory, which lie on the dispersion curves of the first mode in Fig. 3. Once the phase-match points have been calculated, the amplitudes of the second harmonics can be obtained through Eqs. (89) and (94). The phase-match points and the corresponding amplitude coefficients of the second harmonics in Eqs. (89) and (94) are given in Table II. The material constants used here are given by Eq. (58).

Substitution of Eqs. (80), (81), (84) and (88) into Eq. (67) yields the expression for the axial strain as

$$\frac{\partial w^{(1)}}{\partial x} = \Psi_4 \frac{U^2}{h^2}\frac{x}{h}\sin 2(\omega t - kx) - \Psi_5 \frac{U^2}{h^2}\cos 2(\omega t - kx) - \Psi_6 \frac{U^2}{h^2} \tag{93}$$

where the amplitude coefficients in Eq. (93) are given by

$$\begin{aligned}
\Psi_4 &= \left(8\pi^2 \frac{1-\nu}{\nu\bar{h}}\delta^2 n^2 - \frac{64}{3}\pi^4 \frac{\delta^4}{\nu\bar{h}} - \frac{\bar{h}}{\nu}\right)\Psi_3 \\
\Psi_5 &= \frac{64}{3}\pi^3 \frac{\delta^3}{\nu\bar{h}}\Psi_3 + 4\pi^2 \frac{\lambda_2}{\mu\bar{h}}\frac{1-\nu}{\nu}\delta^2\Gamma_2 + \frac{1-\nu}{4\nu}\frac{\lambda_2}{\mu}\Gamma_3 \\
\Psi_6 &= \frac{1-\nu}{4\nu}\frac{\lambda_2}{\mu}\Gamma_3
\end{aligned} \tag{94}$$

As the propagation distance increases, the cumulative second harmonic with the amplitude coefficient Ψ_4 will be dominant in Eq. (93).

TABLE II. The phase-match points and the corresponding coefficients of the amplitudes of second harmonics

h/R	$\delta = h/\lambda$	$n = c/c_T$	Ψ_3	Ψ_4	Ψ_5	Ψ_6
1/10	0.065	0.445	1.80×10^{-2}	-5.11×10^{-4}	-2.80×10^{-3}	-8.77×10^{-2}
1/30	0.037	0.252	2.45×10^{-3}	-3.67×10^{-5}	-1.53×10^{-4}	-9.34×10^{-3}

From Table II, we observe that the amplitudes of second harmonics in the thinner-walled pipe are smaller than the amplitudes of second harmonics in the thicker-walled pipe. That means a lower power flux from the primary wave to the second harmonic occurs in the thinner pipe.

To validate the analysis in this section, the phase-match point lying on the dispersion curve of first mode is compared with the corresponding point given by Liu *et al*. (2013b). The ratio of thickness to mean radius is 150/975. Our result is ($\delta = 0.080$, $n = 0.546$) compared with the result of Liu *et al*. ($\delta = 0.086$, $n = 0.536$). The discrepancy between the two results is small.

5. Conclusions

In this paper, guided waves propagating in pipes with quadratic material nonlinearity have been investigated. The paper is composed of three main parts: the derivation of the shell equations, the mixing of longitudinal and torsional waves, and the self-interaction of longitudinal waves. Analytical expressions of cumulative second harmonics have been obtained based on shell theory.

The derivation of governing equations of axisymmetric motion of a pipe with nonlinear material behavior has been given in the first part. By use of the perturbation method, the zero and first order equations have been derived. The dispersion curves obtained from the linear version of the present theory, the linear thick shell theory and the linear three dimensional theory show excellent agreement. It was shown that no resonant longitudinal harmonic with sum or difference frequency exists. Analytical expressions of the resonant torsional harmonics with difference and sum frequencies were obtained. The resonant torsional harmonics generated by the mixing of longitudinal and torsional waves propagate in the opposite direction of the primary wave.

For thin-walled shells, the shell theory has been further simplified to yield uncoupled linear and nonlinear parts of the governing equations. The simplified shell theory has been used to analytically investigate the self-interaction of longitudinal waves in thin-walled pipes. To validate the thin shell theory, the dispersion curves for longitudinal waves were compared with the corresponding curves obtained from thick shell theory. It was shown that the dispersion curves agree very well with each other when the ratio of thickness to wavelength is small. For second longitudinal harmonics in pipes, analytical expressions for the phase-match conditions are presented, which together with the corresponding dispersion relation, have been used to

determine the phase-match points. The analytical solutions presented in this paper may provide a benchmark to numerical and experimental investigations.

Acknowledgements

The work was supported by the National Natural Science Foundation of China (Nos. 11272281 and 11532001) and the China Scholarship Council (CSC). Partial support from the Fundamental Research Funds for the Central Universities (No. 2016XZZX001-05) is also acknowledged.

Appendix A:

In cylindrical coordinates, the nonlinear parts of the Cauchy stress components only including quadratic material nonlinearity for axisymmetric wave fields are given by (Wang and Achenbach, 2016)

$$\sigma_{rr}^{NL}=(B+C)\left(\frac{\overline{u}^2}{\overline{r}^2}+\overline{w}_{,x}^2\right)+2C\frac{\overline{u}\overline{w}_{,x}}{\overline{r}}+(2B+2C)\left(\frac{\overline{u}\overline{u}_{,r}}{\overline{r}}+\overline{u}_{,r}\overline{w}_{,x}\right)+(A+3B+C)\overline{u}_{,r}^2 +\frac{1}{2}B\overline{v}_{,x}^2+\left(\frac{1}{4}A+\frac{1}{2}B\right)\left(\overline{u}_{,x}^2+\frac{\overline{v}^2}{\overline{r}^2}+\overline{w}_{,r}^2+\overline{v}_{,r}^2\right)+\left(\frac{1}{2}A+B\right)\left(\overline{u}_{,x}\overline{w}_{,r}-\frac{\overline{v}\overline{v}_{,r}}{\overline{r}}\right) \tag{A1}$$

$$\sigma_{r\theta}^{NL}=\left(\frac{1}{2}A+B\right)\left(\overline{u}_{,r}\overline{v}_{,r}-\frac{\overline{u}\overline{v}}{\overline{r}^2}+\frac{\overline{u}\overline{v}_{,r}}{\overline{r}}-\frac{\overline{v}\overline{u}_{,r}}{\overline{r}}\right)+\frac{1}{4}A\left(\overline{u}_{,x}\overline{v}_{,x}+\overline{v}_{,x}\overline{w}_{,r}\right)+B\left(\overline{v}_{,r}\overline{w}_{,x}-\frac{\overline{v}\overline{w}_{,x}}{\overline{r}}\right) \tag{A2}$$

$$\sigma_{rx}^{NL}=\left(\frac{1}{2}A+B\right)\left(\overline{u}_{,r}\overline{u}_{,x}+\overline{w}_{,r}\overline{w}_{,x}+\overline{u}_{,r}\overline{w}_{,r}+\overline{u}_{,x}\overline{w}_{,x}\right)+\frac{A}{4}\left(\overline{v}_{,r}\overline{v}_{,x}-\frac{\overline{v}\overline{v}_{,x}}{\overline{r}}\right)+B\left(\frac{\overline{u}\overline{u}_{,x}}{\overline{r}}+\frac{\overline{u}\overline{w}_{,r}}{\overline{r}}\right) \tag{A3}$$

$$\sigma_{\theta\theta}^{NL}=(A+3B+C)\frac{\overline{u}^2}{\overline{r}^2}+B\overline{u}_{,x}\overline{w}_{,r}+2C\overline{u}_{,r}\overline{w}_{,x}+(2B+2C)\left(\frac{\overline{u}\overline{u}_{,r}}{\overline{r}}+\frac{\overline{u}\overline{w}_{,x}}{\overline{r}}\right)+(B+C)\left(\overline{u}_{,r}^2+\overline{w}_{,x}^2\right) +\frac{1}{2}B\left(\overline{u}_{,x}^2+\overline{w}_{,r}^2\right)-\left(\frac{A}{2}+B\right)\frac{\overline{v}\overline{v}_{,r}}{\overline{r}}+\left(\frac{A}{4}+\frac{1}{2}B\right)\left(\frac{\overline{v}^2}{\overline{r}^2}+\overline{v}_{,r}^2+\overline{v}_{,x}^2\right) \tag{A4}$$

$$\sigma_{\theta x}^{NL}=\frac{1}{4}A\left(\bar{u}_{,x}\bar{v}_{,r}-\frac{\overline{vw}_{,r}}{\bar{r}}+\bar{v}_{,r}\bar{w}_{,r}-\frac{\overline{vu}_{,x}}{\bar{r}}\right)+\left(\frac{A}{2}+B\right)\left(\frac{\overline{uv}_{,x}}{\bar{r}}+\bar{v}_{,x}\bar{w}_{,x}\right)+B\bar{u}_{,r}\bar{v}_{,x} \tag{A5}$$

$$\begin{aligned}\sigma_{xx}^{NL}=&\left(A+3B+C\right)\bar{w}_{,x}^{2}+\left(B+C\right)\left(\frac{\bar{u}^{2}}{\bar{r}^{2}}+\bar{u}_{,r}^{2}\right)+2C\frac{\overline{uu}_{,r}}{\bar{r}}-B\frac{\overline{vv}_{,r}}{\bar{r}}+\frac{B}{2}\left(\frac{\bar{v}^{2}}{\bar{r}^{2}}+\bar{v}_{,r}^{2}\right)\\&+\left(\frac{1}{4}A+\frac{1}{2}B\right)\left(\bar{u}_{,x}^{2}+\bar{v}_{,x}^{2}+\bar{w}_{,r}^{2}+2\bar{u}_{,x}\bar{w}_{,r}\right)+\left(2B+2C\right)\left(\frac{\overline{uw}_{,x}}{\bar{r}}+\bar{u}_{,r}\bar{w}_{,x}\right)\end{aligned} \tag{A6}$$

Equations. (A1)-(A6) can also be reduced from the corresponding equations in Liu *et al*. (2013a) if we only consider axisymmetric motion with small deformations (but considering material nonlinearities). The subscript letter following the comma denotes the corresponding differential derivative.

References

Hikata A., Chick B.B., Elbaum C., 1965. Dislocation contribution to the second harmonic generation of ultrasonic waves. J. Appl. Phys. 229-236

Hikata A., Sewell J.F.A., Elbaum C., 1966. Generation of ultrasonic second and third harmonics due to dislocations. II. Phys. Rev., 442-449

Deng M., Wang P., Lv X., 2005. Experimental observation of cumulative second-harmonic generation of Lamb-wave propagation in an elastic plate. J. Phys. D: Appl. Phys. 344-353

Zhang Z., Liu D., Deng M., Ta D., Wang W., 2014. Experimental observation of cumulative second-harmonic generation of lamb waves propagating in long bones. Ultrasound Med. Biol. 1660-1670

Bermes C., Kim J.Y., Qu J., Jacobs L.J., 2007. Experimental characterization of material nonlinearity using Lamb waves. Appl. Phys. Lett. 021901

Gol'dberg Z.A., 1961. Interaction of plane longitudinal and transverse elastic waves. Sov. Phys. Acoust. 306-310

Bender F.A., Kim J.Y., Jacobs L.J., Qu J., 2013. The generation of second harmonic waves in an isotropic solid with quadratic nonlinearity under the presence of a stress-free boundary. Wave Motion 146-161

Matlack K.H., Kim J.Y., Jacobs L.J., Qu J., 2015. Review of second harmonic generation measurement techniques for material state determination in metals. J. Nondestr. Eval. 1-23

Chen Z., Tang G., Zhao Y., Jacobs L.J., Qu J., 2014. Mixing of collinear plane wave pulses in elastic solids with quadratic nonlinearity. J. Acoust. Soc. Am. 2389-2404

Deng M., 1998. Cumulative second-harmonic generation accompanying nonlinear shear horizontal mode propagation in a solid plate. J. Appl. Phys. 3500-3505

Deng M., 1999. Cumulative second-harmonic generation of Lamb-mode propagation in a solid plate," J. Appl. Phys. 3051-3058

Pau A., Scalea F.L.di., 2015. Nonlinear guided wave propagation in prestressed plates. J. Acoust. Soc. Am. 1529-1540

de Lima W.J.N., Hamilton M. F., 2003. Finite-amplitude waves in isotropic elastic plates. J. Sound Vib. 819-839

de Lima W.J.N., Hamilton M.F., 2005. Finite amplitude waves in isotropic elastic waveguides with arbitrary constant cross-sectional area. Wave Motion 1-11

Liu Y., Lissenden C.J., Rose J.L., 2014a. Higher order interaction of elastic waves in weakly nonlinear hollow circular cylinders. I. Analytical foundation. J. Appl. Phys. 214901

Liu Y., Khajeh E., Lissenden C.J., Rose J.L., 2014b. Higher order interaction of elastic waves in weakly nonlinear hollow circular cylinders. II. Physical interpretation and numerical results. J. Appl. Phys. 214902

Liu Y., Khajeh E., Lissenden C.J., Rose J.L., 2013a. Interaction of torsional and longitudinal guided waves in weakly nonlinear circular cylinders. J. Acoust. Soc. Am. 2541-2553

Liu, Y., Lissenden, C.J., Rose, J.L., 2013b. Cumulative second harmonics in weakly nonlinear plates and shells. In: Kundu, T. (ed), Health Monitoring of Structural and Biological Systems. Proceedings of SPIE, San Diego, pp. 86950S–86950S-12

Chillara V.K., Lissenden C.J., 2013. Analysis of second harmonic guided waves in pipes using a large-radius asymptotic approximation for axis-symmetric longitudinal modes. Ultrasonics 862-869

Wang Y., Zhang C., Dai H.-H., Chen W., 2015a. Adjustable solitary waves in electroactive rods. J. Sound Vib. 188-207

Wang Y., Dai H.-H., Chen W., 2015b. Kink and kink-like waves in pre-stretched Mooney-Rivlin viscoelastic rods. AIP Adv. 087167

Morsbøl J., Sorokin S.V., 2015. Elastic wave propagation in curved flexible pipes. Int. J. Solids Struct. 143-155

Herrmann G. and Mirsky I., 1956. Three-dimensional and shell-theory analysis of axially symmetric motions of cylinders. J. Appl. Mech. 563 – 568

Wang Y., Achenbach J.D., 2016. The effect of cubic material nonlinearity on the propagation of torsional wave modes in a pipe. J. Acoust. Soc. Am. 3874-3883

Achenbach J.D., 1999. Wave Propagation in Elastic Solids. North Holland, Amsterdam.

Mirsky I., Herrmann G., 1958. Axially motions of thick cylindrical shells. J. Appl. Mech. 97-102

Li J., Rose J.L., 2006. Natural beam focusing of non-axisymmetric guided waves in large-diameter pipes. Ultrasonics 35-45

Korneev V.A., Demčenko A., 2014. Possible second-order nonlinear interactions of plane waves in an elastic solid. J. Acoust. Soc. Am. 591-598

Junger M.C., Feit D., 1986. Sound, Structures, and Their interaction, second ed. MIT press, Cambridge.